

QCD quark cyclobutadiene and light tetraquark spectraChengrong Deng,¹ Jialun Ping,^{2,*} Hui Wang,² Ping Zhou,¹ and Fan Wang³¹*School of Mathematics and Physics, Chongqing Jiaotong University, Chongqing 400074, People's Republic of China*²*Department of Physics, Nanjing Normal University, Nanjing 210097, People's Republic of China*³*Department of Physics, Nanjing University, Nanjing 210093, People's Republic of China*

(Received 19 February 2012; published 21 December 2012)

The QCD quark cyclobutadiene (ringlike), a new color structure of a tetraquark system, is proposed and studied in the flux-tube model with a multibody confinement interaction. Numerical calculations show that the light tetraquark systems (u , d , s only) with cyclobutadiene, diquark-antidiquark flux-tube structures have similar energies and they can be regarded as QCD isomeric compounds. The energies of some tetraquark states are close to the energies of some excited mesons, and so in the study of these mesons, the tetraquark components should be taken into account. There are also some meson states, σ , $\kappa(800)$, $f_0(980)$, $f_0(1500)$, $\pi_1(1400)$, $\pi_1(1600)$, $f_2(1430)$ and $K^*(1410)$, where tetraquark components might be dominant. The meson states with exotic quantum numbers are studied as the tetraquark states. The multibody confinement interaction reduces the energy of the tetraquark state in comparison with the usual additive two-body confinement interaction model.

DOI: [10.1103/PhysRevD.86.114035](https://doi.org/10.1103/PhysRevD.86.114035)

PACS numbers: 14.20.Pt, 12.40.-y

I. INTRODUCTION

In the constituent quark model (CQM), mesons are assumed to be composed of $q\bar{q}$. Although various properties of light mesons have been explained within this $q\bar{q}$ minimum Fock space, there are still properties of some meson states that cannot be described well by this quark model [1–3]. In fact, mesons might be more complicated objects with higher Fock components, other than the lowest $q\bar{q}$. The wave function of a zero baryon number ($B = 0$) hadron, if the gluon degree of freedom is neglected, can be given, in general, as

$$|B = 0\rangle = \sum_n c_n |q^n \bar{q}^n\rangle, \quad (1)$$

where $n = 1, 2, 3, \dots$; the high Fock component $q^2\bar{q}^2$ was taken into account in the investigations of the properties of the low-lying scalar mesons [4–10]. Recent studies on meson spectroscopy called for unquenching the quark model, i.e., the $q\bar{q}$ and $q^2\bar{q}^2$ mixing [3,11–13]. Furthermore, the introduction of tetraquark states $q^2\bar{q}^2$ is indispensable for the states with exotic quantum numbers [14–18]. In recent years, comprehensive research on tetraquark states has been carried out by many authors [19–28]; Belle, BABAR, and other experimental collaborations have observed many open and hidden charmed hadrons, which are difficult to fit into the conventional meson $c\bar{c}$ spectra [29]. The states with quantum numbers $J^{PC} = 0^{--}$, even $^{+-}$ and odd $^{-+}$ have been theoretically studied as tetraquark states [30–32]. Experimental evidence of exotic states with quantum numbers $J^{PC} = 1^{-+}$ has been accumulated [14–18]. The investigations of multi-quark states with flux-tube structures will provide important low energy

quantum chromodynamics (QCD) information, such as $q\bar{q}^2$ and $q^2\bar{q}$ interactions [33], which is absent in ordinary hadrons due to their unique flux-tube structure.

QCD is widely accepted as the fundamental theory of a strong interaction, in which color confinement is a long-distance behavior whose understanding continues to be a challenge in theoretical physics. Lattice QCD (LQCD) allows us to investigate the confinement phenomenon in a nonperturbative framework, and its calculations on mesons, baryons, and tetraquark and pentaquark states reveal flux-tube or stringlike structures [34–37]. Such flux-tube—like structures lead to a “phenomenological” understanding of color confinement and, naturally, to a linear confinement potential in $q\bar{q}$ and q^3 quark systems.

It is well known that nuclear force and molecule force are very similar except for the length and energy scale difference [38,39]. For multibody systems, the flux tubes in a multi-quark system should also be very similar to the chemical bond in the molecular system. Among organic compounds, the same molecular constituents may have different chemical bond structure; these are called isomeric compounds. In the hadronic world, multi-quark states with the same quark content but different flux-tube structures are similarly called QCD isomeric compounds. The past theoretical studies on multi-quark states reveal various flux-tube structures [40–49]: hadron molecular states $[q\bar{q}]_1[q\bar{q}]_1$, $[q\bar{q}]_1[q^3]_1$, $[q^3]_1[q^3]_1$ and $[\bar{q}^3]_1[q^3]_1$ and hidden color states $[[q\bar{q}]_8[q\bar{q}]_8]_1$, $[[q^2]_3[\bar{q}^2]_3]_1$, $[[q\bar{q}]_8[q^3]_8]_1$, $[[q^2]_3[q^2]_3\bar{q}]_1$, $[[q^4]_3\bar{q}]_1$, $[[q^3]_8[q^3]_8]_1$, $[[q^2]_3[q^2]_3[q^2]_3]_1$, $[[\bar{q}^3]_8[q^3]_8]_1$ and a QCD quark benzene $[q^6]_1$, *et al.*; here the subscripts represent color dimensions, which should be mixed, and they affect the corresponding hadron properties if they really exist.

Based on the chemical benzene and the similarity between color flux tubes and chemical bonds, a new

*Corresponding author.
jlping@njnu.edu.cn

flux-tube structure, the quark benzene, for a six-quark system was proposed, and its possible effect on NN scattering was discussed in our previous paper [48]. In the present work, a new flux-tube structure for a tetraquark state, which is similar to the molecular cyclobutadiene and is therefore called QCD quark cyclobutadiene, is proposed. The aims of this paper are as follows: (i) to investigate the properties of a QCD cyclobutadiene in the flux-tube model, which involves a multibody confinement potential and has been successfully applied to multi-quark systems [49,50]; (ii) to study the spectra of light tetraquark states with two flux-tube structures (diquark-antidiquark and QCD quark cyclobutadiene), which helps us to understand the meson states beyond a $q\bar{q}$ configuration and will provide a new sample to study the mixing of $q\bar{q}$ and $q^2\bar{q}^2$. The research shows that (i) the light tetraquark states with cyclobutadiene, diquark-antidiquark flux-tube structures have similar energies, and they can be regarded as QCD isomeric compounds; (ii) most of the experimentally observed mesons can be interpreted as $q\bar{q}$ states (at least the main component) and accommodated in the naive quark model. Only a few of them may go beyond $q\bar{q}$ configurations and be explained by their dominant components as tetraquark states; the masses of some tetraquark states are close to the masses of some excited mesons, and so the tetraquark components should be taken into account in the description of the properties of the mesons.

The paper is organized as follows: four possible flux-tube structures of a tetraquark system are discussed in Sec. II. Section III is devoted to the descriptions of the flux-tube model and the multibody confinement potentials of diquark-antidiquark and QCD quark cyclobutadiene structures. A brief introduction of the construction of the wave functions and quantum numbers of a tetraquark state is given in Sec. IV. The numerical results and discussions are presented in Sec. V. A brief summary is given in the last section.

II. FLUX-TUBE STRUCTURES OF A TETRAQUARK STATE

In the flux-tube picture it is assumed that the color-electric flux is confined to narrow, flux-tube—like tubes joining quarks and antiquarks. A flux tube starts from each quark and ends at an antiquark or a Y -shaped junction, where three flux tubes are either annihilated or created [51]. In general, a state with $N + 1$ particles can be generated by replacing a quark or an antiquark in an N -particle state by a Y -shaped junction and two antiquarks or two quarks. According to this point of view, there are four possible flux-tube structures for a tetraquark system, as shown in Fig. 1, where \mathbf{r}_i represents the position of a quark q_i (antiquark \bar{q}_i) which is denoted by a solid (hollow) dot, and \mathbf{y}_i represents a junction where three flux tubes meet. A thin line connecting a quark and a junction represents a fundamental flux tube, i.e., a color triplet. A thick line

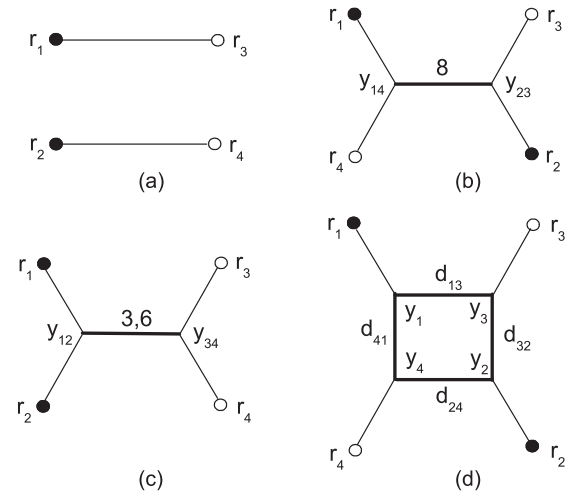


FIG. 1. Four possible flux-tube structures.

connecting two junctions is for a color sextet, octet or others, namely, a compound flux tube. The numbers on the flux tubes represent the color dimensions of the corresponding flux tube. The different types of flux tubes may have different stiffness [52]; details will be discussed in the next section. Both the overall color singlet nature of a multi-quark system and the $SU(3)$ color coupling rule at each junction must be satisfied.

The flux-tube structure in Fig. 1(a) is a meson-meson molecule state; many newly observed exotic hadrons are discussed in this picture [40–42]. The tetraquark states with flux-tube structure [Fig. 1(b)] generally have high energies due to a repulsive interaction between a quark and an antiquark in a color octet meson. Thus, this flux-tube structure is often neglected in the study of multi-quark states. However, sometimes the attraction between two color octet mesons will lower the energies of the system considerably. In the case of the flux-tube structure [Fig. 1(c)], called diquark-antidiquark structure, it has two possible color coupling schemes, namely, $[[qq]_3[\bar{q}\bar{q}]_3]_1$ and $[[qq]_6 \times [\bar{q}\bar{q}]_6]_1$; the latter is expected to be a highly excited state, and therefore, the diquark $[qq]_6$ is usually called the “bad” diquark, since the interaction between two symmetric quarks (antiquarks) is repulsive. Thus, many authors are in favor of the “good” diquark $[qq]_3$ picture [43–45].

The first three flux-tube structures can be explained as the basic structures for a tetraquark system. The last structure can be generated by means of exciting two Y -shaped junctions and three compound flux tubes from vacuum based on the second or third structures. In the CQM, a quark is massive. One can suppose that the recombination of flux tubes is faster than the motion of the quarks. Subsequently, the ends of four compound flux tubes meet each other in turn to form a closed flux-tube structure, a ring- $\mathbf{y}_1\mathbf{y}_3\mathbf{y}_2\mathbf{y}_4$, which was interpreted as a pure gluon state by Isgur and Paton [51], and as a glueball state in the framework of the dual Ginzburg-Landau theory [53].

With quarks or antiquarks connecting to the vertex y_i by a fundamental flux tube, where $i = 1, 2, 3, 4$, this picture could be explained as a $q^2\bar{q}^2$ -glueball hybrid. According to the overall color singlet and $SU(3)$ color coupling rule, the corresponding compound color flux-tube dimensions $(d_{13}, d_{32}, d_{24}, d_{41})$ have six different sets: $(3, 8, 3, 8)$, $(\bar{6}, 8, \bar{6}, 8)$, $(\bar{3}, 3, \bar{3}, 3)$, $(8, \bar{3}, 8, \bar{3})$, $(8, 6, 8, 6)$ and $(\bar{3}, \bar{6}, \bar{3}, \bar{6})$. The flux tubes located on opposite sides of the ring- $y_1y_3y_2y_4$ have the same color dimensions, which is similar to the symmetry of the distribution of double bonds and single bonds in a cyclobutadiene in chemistry. We thus call the flux-tube structure [Fig. 1(d)] a QCD quark cyclobutadiene. Of course, the existence of another QCD quark cyclobutadiene in which two quarks or antiquarks are neighbors in the flux-tube ring is also allowed. Certainly, more complicated configurations are permitted, including more Y -shaped junctions and more complex topological structures.

III. THE FLUX-TUBE MODEL AND MULTIBODY CONFINEMENT POTENTIALS

Recently, LQCD and nonperturbative QCD methods have made impressive progress on hadron properties, even on hadron-hadron interactions [54–58]. However, the QCD-inspired CQM is still a useful tool in obtaining physical insight for these complicated strong interaction systems. The CQM can offer the most complete description of hadron properties and is probably the most successful phenomenological model of hadron structure [1]. In the traditional CQM, a two-body interaction proportional to the color charges $\lambda_i \cdot \lambda_j$ and r_{ij}^n , where $n = 1$ or 2 and r_{ij} is the distance between two quarks, was introduced to phenomenologically describe the quark confinement interaction. The traditional model can well describe the properties of ordinary hadrons (q^3 and $q\bar{q}$) because the flux-tube structures for an ordinary hadron are unique and trivial. However, the traditional model is known to be flawed phenomenologically because it leads to power-law Van der Waals forces between color singlet hadrons [59–61]. It is also flawed theoretically in that it is very implausible that the long-range static multibody potential is just a sum of the two-body ones [62]. Many papers were devoted to eliminating the physically nonexistent long-distance Van der Waals force arising from the traditional models based on the sum of two-body Casimir scaled potentials [63–66].

LQCD studies show that the confinement potential of a multi-quark state is a multibody interaction which is proportional to the minimum of the total length of flux tubes which connects the quarks to form a multi-quark state [34–37]. The naive flux-tube model is developed based on the LQCD picture by taking into account a multibody confinement potential with a harmonic interaction approximation; i.e., a sum of the square of the length of flux tubes rather than a linear one is assumed to simplify

the calculation [48,67]. The approximation is justified because of the following two reasons: one is that the spatial variations in separation of the quarks (lengths of the flux tube) in different hadrons do not differ significantly, so the difference between the two functional forms is small and can be absorbed in the adjustable parameter, the stiffness. The other is that we are using a nonrelativistic dynamics in the study. As was shown long ago [68], an interaction energy that varies linearly with separation between fermions in a relativistic first order differential dynamics has a wide region in which a harmonic approximation is valid for the second order (Feynman-Gell-Mann) reduction of the equations of motion. Combining with the Gaussian expansion method (GEM), the flux-tube model, including one gluon exchange and one boson exchange interactions, was successfully applied to new hadronic states, and some interesting results were obtained [49,50].

Within the flux-tube picture, the flux tubes in the ring structure [see Fig. 1(d)] are assumed to have the same properties as the flux tubes in the ordinary meson or baryon [69]. Thus, in the flux-tube model with quadratic confinement, the confinement potentials V^c and V^d for diquark-antidiquark and cyclobutadiene structures have the following forms, respectively:

$$V^c = k[(\mathbf{r}_1 - \mathbf{y}_1)^2 + (\mathbf{r}_2 - \mathbf{y}_1)^2 + (\mathbf{r}_3 - \mathbf{y}_2)^2 + (\mathbf{r}_4 - \mathbf{y}_2)^2 + \kappa_{d_{12}}(\mathbf{y}_1 - \mathbf{y}_2)^2], \quad (2)$$

$$V^d = k \left[\sum_{i=1}^4 (\mathbf{r}_i - \mathbf{y}_i)^2 + \sum'_{i<j} \kappa_{d_{ij}} (\mathbf{y}_i - \mathbf{y}_j)^2 \right], \quad (3)$$

where the \sum' means that the summation is over the adjacent junction pairs on a compound flux tube; this term is the energy of the flux-tube ring- $y_1y_3y_2y_4$. The parameter k is the stiffness of an elementary flux tube, while $k\kappa_{d_{ij}}$ is other compound flux-tube stiffness. The compound flux-tube stiffness parameter $\kappa_{d_{ij}}$ depends on the color dimension, d_{ij} , of the flux tube [52],

$$\kappa_{d_{ij}} = \frac{C_{d_{ij}}}{C_3}, \quad (4)$$

where $C_{d_{ij}}$ is the eigenvalue of the Casimir operator associated with the $SU(3)$ color representation d_{ij} on either end of the flux tube, namely, $C_3 = \frac{4}{3}$, $C_6 = \frac{10}{3}$ and $C_8 = 3$.

For given quark positions \mathbf{r}_i , the positions of those junctions \mathbf{y}_i , variational parameters, can be determined by means of minimizing the confinement potentials V^c and V^d . To simplify the formats of V^c and V^d after obtaining the positions of the junctions \mathbf{y}_i , two sets of canonical coordinates \mathbf{R}_i and \mathcal{R}_i can be introduced, respectively, and be written as

$$\begin{pmatrix} \mathbf{R}_1 \\ \mathbf{R}_2 \\ \mathbf{R}_3 \\ \mathbf{R}_4 \end{pmatrix} = \begin{pmatrix} \frac{1}{\sqrt{2}} & \frac{-1}{\sqrt{2}} & 0 & 0 \\ 0 & 0 & \frac{1}{\sqrt{2}} & \frac{-1}{\sqrt{2}} \\ \frac{1}{\sqrt{4}} & \frac{1}{\sqrt{4}} & \frac{-1}{\sqrt{4}} & \frac{-1}{\sqrt{4}} \\ \frac{1}{\sqrt{4}} & \frac{1}{\sqrt{4}} & \frac{1}{\sqrt{4}} & \frac{1}{\sqrt{4}} \end{pmatrix} \begin{pmatrix} \mathbf{r}_1 \\ \mathbf{r}_2 \\ \mathbf{r}_3 \\ \mathbf{r}_4 \end{pmatrix} \quad (5)$$

$$\begin{pmatrix} \mathcal{R}_1 \\ \mathcal{R}_2 \\ \mathcal{R}_3 \\ \mathcal{R}_4 \end{pmatrix} = \begin{pmatrix} \frac{1}{\sqrt{4}} & \frac{-1}{\sqrt{4}} & \frac{-1}{\sqrt{4}} & \frac{1}{\sqrt{4}} \\ \frac{1}{\sqrt{4}} & \frac{1}{\sqrt{4}} & \frac{-1}{\sqrt{4}} & \frac{-1}{\sqrt{4}} \\ \frac{1}{\sqrt{4}} & \frac{-1}{\sqrt{4}} & \frac{1}{\sqrt{4}} & \frac{-1}{\sqrt{4}} \\ \frac{1}{\sqrt{4}} & \frac{1}{\sqrt{4}} & \frac{1}{\sqrt{4}} & \frac{1}{\sqrt{4}} \end{pmatrix} \begin{pmatrix} \mathbf{r}_1 \\ \mathbf{r}_2 \\ \mathbf{r}_3 \\ \mathbf{r}_4 \end{pmatrix}.$$

The minimums V_{\min}^c and V_{\min}^d of the confinement potentials can be divided into three independent harmonic oscillators and therefore have the following forms,

$$V_{\min}^c = k \left[\mathbf{R}_1^2 + \mathbf{R}_2^2 + \frac{\kappa_{d_{12}}}{1 + \kappa_{d_{12}}} \mathbf{R}_3^2 \right] \quad (7)$$

$$V_{\min}^d = k \left[\frac{2\kappa_{d_1}}{1 + 2\kappa_{d_1}} \mathcal{R}_1^2 + \frac{2\kappa_{d_2}}{1 + 2\kappa_{d_2}} \mathcal{R}_2^2 + \frac{2(\kappa_{d_1} + \kappa_{d_2})}{1 + 2(\kappa_{d_1} + \kappa_{d_2})} \mathcal{R}_3^2 \right], \quad (8)$$

where the parameters κ_{d_1} and κ_{d_2} are used to describe the stiffness of two sets of opposite flux tubes in the ring- $\mathbf{y}_1\mathbf{y}_3\mathbf{y}_2\mathbf{y}_4$ due to the symmetry, respectively. Obviously, the confinement potentials V_{\min}^c and V_{\min}^d are multibody interactions rather than the sum of two-body interactions.

The limit $\kappa_{d_{ij}}$ going to infinity indicates that the corresponding compound flux tube contracts to a junction due to the requirement of the minimum of the confinement. The limit $\kappa_{d_{ij}}$ going to zero indicates the rupture of the corresponding compound flux tube, and then a multi-quark state decays into several color singlet hadrons. The flux-tube structures of a multi-quark state can therefore change if the $\kappa_{d_{ij}}$ is taken as an adjustable parameter. In the limit where κ_{d_1} or κ_{d_2} goes to infinity, a QCD quark cyclobutadiene reduces to a two color octet meson state or a diquark-antidiquark state. In the limit where κ_{d_1} or κ_{d_2} goes to infinity and the other goes to zero, a QCD quark cyclobutadiene decays into two color singlet meson states. In the limit where all κ_d 's in Fig. 1 go to infinity, the last three flux-tube structures reduce to one structure because all compound flux tubes shrink to a junction, leaving a hub and spokes configuration.

Taking into account a potential energy shift Δ in each independent harmonic oscillator, the confinement potentials V_{\min}^c and V_{\min}^d have, therefore, the following forms:

$$V_{\min}^c = k \left[(\mathbf{R}_1^2 - \Delta) + (\mathbf{R}_2^2 - \Delta) + \frac{\kappa_{d_{12}}}{1 + \kappa_{d_{12}}} (\mathbf{R}_3^2 - \Delta) \right] \quad (9)$$

$$V_{\min}^d = k \left[\frac{2\kappa_{d_1}}{1 + 2\kappa_{d_1}} (\mathcal{R}_1^2 - \Delta) + \frac{2\kappa_{d_2}}{1 + 2\kappa_{d_2}} (\mathcal{R}_2^2 - \Delta) + \frac{2(\kappa_{d_1} + \kappa_{d_2})}{1 + 2(\kappa_{d_1} + \kappa_{d_2})} (\mathcal{R}_3^2 - \Delta) \right], \quad (10)$$

where the parameters k and Δ are determined by fitting ordinary meson spectra [50]. Carlson and Pandharipande also considered a similar flux-tube energy shift which is proportional to the number of quarks N [70].

One gluon exchange and one Goldstone boson exchange interactions are not only important and responsible for the mass splitting in the ordinary hadron spectra, but are also indispensable for the investigations on the multi-quark system [49]; the details of the parts of the Hamiltonian model can be found in our previous paper [50].

IV. WAVE FUNCTIONS AND DEFINITION OF QUANTUM NUMBERS

The flux-tube structure specifies how the colors of quarks and antiquarks are coupled to form an overall color singlet. It is, however, difficult to construct the color wave function of the QCD quark cyclobutadiene only using quark degrees of freedom in the framework of the quark models. In order to comprehensively study a QCD quark cyclobutadiene, one gluon exchange and one boson exchange interactions have to be included. The color wave function of a QCD quark cyclobutadiene is therefore indispensable and approximately assumed to be the same as that of a diquark-antidiquark structure. In the framework of a diquark-antidiquark structure, three relative motions are shown in Fig. 2, where \mathbf{r}_i represents the position of the quark q_i (antiquark \bar{q}_i) which is denoted by a solid (hollow) dot. The corresponding Jacobi coordinates can be expressed as

$$\begin{aligned} \mathbf{r} &= \mathbf{r}_1 - \mathbf{r}_2, & \mathbf{R} &= \mathbf{r}_3 - \mathbf{r}_4, \\ \mathbf{X} &= \frac{m_1\mathbf{r}_1 + m_2\mathbf{r}_2}{m_1 + m_2} - \frac{m_3\mathbf{r}_3 + m_4\mathbf{r}_4}{m_3 + m_4}. \end{aligned} \quad (11)$$

L , l_1 and l_2 are the orbital angular momenta associated with the relative motion coordinates \mathbf{X} , \mathbf{r} and \mathbf{R} ,

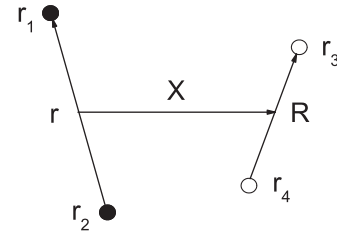


FIG. 2. Jacobi coordinates for a $q^2\bar{q}^2$ system.

respectively. The total wave function of a tetraquark state can be written as a sum of the following direct products of color, isospin, spin and spatial terms,

$$\Phi_{IJ}^{q^2\bar{q}^2} = \sum_{\alpha} \xi_{\alpha}^{IJ} [[\phi_{l_1}^G(\mathbf{r})\chi_{s_1}]_{J_1} [\psi_{l_2}^G(\mathbf{R})\chi_{s_2}]_{J_2}]_{J_{12}} F_L^G(\mathbf{X})_J \times [\eta_{l_1}\eta_{l_2}]_I [\chi_{c_1}\chi_{c_2}]_C, \quad (12)$$

where I and J are total isospin and angular momentum, respectively. α represents all possible intermediate quantum numbers, $\alpha = \{l_i, s_i, J_i, J_{12}, L, I_i\}$, where $i = 1, 2$. χ_{s_i} , η_{l_i} and χ_{c_i} are spin, flavor and color wave functions of a diquark or an antidiquark, respectively. $[\]_s$ denote Clebsch-Gordan coefficient coupling. The overall color singlet can be constructed in two ways: $\chi_c^1 = \bar{3}_{12} \otimes 3_{34}$, $\chi_c^2 = 6_{12} \otimes \bar{6}_{34}$. The ‘‘good’’ diquark and the ‘‘bad’’ diquark are both included. Taking into account all degrees of freedom, the Pauli principle must be satisfied for each subsystem of identical quarks or antiquarks. The coefficient ξ_{α}^{IJ} is determined by diagonalizing the Hamiltonian.

To obtain a reliable solution of a few-body problem, a high precision method is indispensable. In this work, the GEM [71], which has been proven to be rather powerful in solving a few-body problem, is used to study four-body systems in the flux-tube model. In the GEM, three relative motion wave functions are expanded as

$$\begin{aligned} \phi_{l_1 m_1}^G(\mathbf{r}) &= \sum_{n_1=1}^{n_{1\max}} c_{n_1} N_{n_1 l_1} r^{l_1} e^{-\nu_{n_1} r^2} Y_{l_1 m_1}(\hat{\mathbf{r}}), \\ \psi_{l_2 m_2}^G(\mathbf{R}) &= \sum_{n_2=1}^{n_{2\max}} c_{n_2} N_{n_2 l_2} R^{l_2} e^{-\nu_{n_2} R^2} Y_{l_2 m_2}(\hat{\mathbf{R}}), \\ F_{LM}^G(\mathbf{X}) &= \sum_{n_3=1}^{n_{3\max}} c_{n_3} N_{LM} X^L e^{-\nu_{n_3} X^2} Y_{LM}(\hat{\mathbf{X}}), \end{aligned} \quad (13)$$

where $N_{n_1 l_1}$, $N_{n_2 l_2}$ and $N_{n_3 l_3}$ are normalization constants. Gaussian size parameters are taken as the following geometric progression numbers:

$$\nu_n = \frac{1}{r_n^2}, \quad r_n = r_1 a^{n-1}, \quad a = \left(\frac{r_{n_{\max}}}{r_1} \right)^{\frac{1}{n_{\max}-1}}. \quad (14)$$

The parity for a diquark-antidiquark state is the product of the intrinsic parities of two quarks and two antiquarks times the factors coming from the spherical harmonics [72],

$$P = P_q P_{\bar{q}} P_{\bar{q}} P_{\bar{q}} (-1)^{l_1+l_2+L} = (-1)^{l_1+l_2+L}. \quad (15)$$

Using our coordinates, the eigenvalues of the charge conjugation of a diquark-antidiquark state can be calculated by following the same steps as in the $q\bar{q}$ case. We can consider a diquark-antidiquark state as a $Q\bar{Q}$ meson, where \bar{Q} and Q represent a diquark and an antidiquark, respectively, with total ‘‘spin’’ J_{12} and relative angular momentum L between Q and \bar{Q} ; see Eq. (12). The C -parity eigenvectors are those states for which Q and \bar{Q} have opposite charges.

So applying the charge conjugation operator to these mesons is the same as exchanging the couple of quarks with the couple of antiquarks. The factors arising from this exchange are the C -parity operator eigenvalues [73],

$$C = (-1)^{L+J_{12}}. \quad (16)$$

The G -parity is a generalization of the concept of C -parity such that members of an isospin multiplet can each be assigned a good quantum number that would reproduce C -parity for the neutral particle. The G -parity operator is defined as the combination of C -parity and a π rotation around the y axis in the isospin space [73],

$$G = C\mathcal{R}_y(\pi) = C e^{i\pi I_2}. \quad (17)$$

The G -parity eigenstates are tetraquark states with flavor charges equal to zero, i.e., strangeness equal to zero in the light meson case, and their eigenvalues are

$$G = (-1)^{L+J_{12}+I}. \quad (18)$$

V. NUMERICAL RESULTS AND DISCUSSIONS

The diquark (antidiquark) is considered as a new compound object \bar{Q} (Q) with no internal spatial excitations, and spatial excitations are assumed to occur only between Q and \bar{Q} in the present numerical calculations, which results in that such a tetraquark state has a lower energy than that of an internal spatial excited one. The orbital angular momenta l_1 and l_2 are therefore assumed to be zero. With these restrictions the intermediate quantum number J_{12} is the total spin angular momentum S . The parity of a tetraquark with the diquark-antidiquark structure is $P = (-1)^L$, the charge conjugation is $C = (-1)^{L+S}$ and the G -parity is $G = (-1)^{L+S+I}$.

Within the flux-tube model with the parameters fixed by fitting the ordinary meson spectra [50], the convergent energies of tetraquark states with this QCD quark cyclobutadiene and diquark-antidiquark structures can be obtained by solving the four-body Schrödinger equation

$$(H - E)\Phi_{IJ}^{q^2\bar{q}^2} = 0, \quad (19)$$

with the Rayleigh-Ritz variational principle, by setting the numbers of the Gaussian wave functions as $n_{1\max} = n_{2\max} = n_{3\max} = 6$. Minimum and maximum ranges of the bases are 0.1 fm and 2.0 fm for Jacobi coordinates \mathbf{r} , \mathbf{R} and \mathbf{X} , respectively. Quark contents with specified quantum numbers $I^G J^{PC}$ or IJ^P and the corresponding masses, in units of MeV, are shown in Tables I, II, III, IV, and V, where n stands for a nonstrange quark (u or d) while s stands for a strange quark; E_I and E_{II} represent the energies of a QCD quark cyclobutadiene and a diquark-antidiquark structure, respectively, and the quantum number N denotes the total radial excitation. The term *exotic* in Tables I and II stands for a meson state which cannot be described by a $q\bar{q}$ configuration.

TABLE I. The mass spectra for $nn\bar{n}\bar{n}$ states.

$I^G J^{PC}$	$N^{2S+1}L_J$	E_I	E_{II}	States	PDG
0^+0^{++}	1^1S_0	601	587	$f_0(600)$	400–1200
0^+0^{++}	2^1S_0	1101	1019	$f_0(980)$	980 ± 10
0^+1^{++}	1^5D_1	1927	1840	$f_1(1285)$	1281.8 ± 0.6
0^+1^{++}	2^5D_1	1984	1919	$f_1(1420)$	1426.4 ± 0.9
0^+1^{++}	3^5D_1	2373	2270	$f_1(1510)$	1518 ± 5
0^+2^{++}	1^1D_2	1328	1196	$f_2(1270)$	1275.1 ± 1.2
0^+2^{++}	2^1D_2	1809	1614	$f_2(1640)$	1639 ± 6
0^+2^{++}	1^5S_2	1468	1465	$f_2(1430)$	≈ 1430
0^+2^{++}	2^5S_2	1495	1508	$f_2'(1525)$	1525 ± 5
0^+2^{++}	1^5D_2	1927	1840	$f_2(1910)$	1903 ± 9
0^+2^{++}	2^5D_2	1984	1919	$f_2(1950)$	1944 ± 12
0^+4^{++}	2^5D_2	1984	1919	$f_4(2050)$	2018 ± 11
0^-2^{+-}	1^3D_2	1908	1836	<i>exotic</i>	...
0^+0^{-+}	1^3P_0	1624	1609	$\eta(1295)$	1294 ± 4
0^+0^{-+}	2^3P_0	1656	1619	$\eta(1405)$	1409.8 ± 2.5
0^+0^{-+}	3^3P_0	2063	2027	$\eta(1475)$	1476 ± 4
0^+0^{-+}	4^3P_0	2097	2055	$\eta(1760)$	1756 ± 9
0^+2^{-+}	1^3P_2	1624	1609	$\eta_2(1645)$	1617 ± 5
0^-1^{--}	1^1P_1	1057	975	$\phi(1020)$	1019.455 ± 0.020
0^-1^{--}	2^1P_1	1482	1358	$\omega(1420)$	1400–1450
0^-1^{--}	3^1P_1	1583	1536	$\omega(1650)$	1670 ± 30
0^-1^{--}	1^5P_1	1696	1651	$\omega(1650)$	1670 ± 30
0^-3^{--}	1^5P_3	1696	1651	$\omega_3(1670)$	1667 ± 4
0^-1^{+-}	1^3S_1	1291	1304	$h_1(1170)$	1170 ± 20
0^-1^{+-}	2^3S_1	1391	1394	$h_1(1380)$	1386 ± 19
1^-0^{++}	1^1S_0	1202	1210	$a_0(980)$	980 ± 20
1^-0^{++}	2^3S_0	1520	1528	$a_0(1450)$	1474 ± 19
1^-1^{++}	1^5D_1	1927	1839	$a_1(1260)$	1230 ± 40
1^-1^{++}	2^5D_1	2373	2271	$a_1(1640)$	1647 ± 22
1^-2^{++}	1^5S_2	1470	1467	$a_2(1320)$	1318.3 ± 0.6
1^-2^{++}	1^1D_2	1876	1807	$a_2(1700)$	1732 ± 16
1^+2^{+-}	1^3D_2	1910	1837	<i>exotic</i>	...
1^-0^{-+}	1^3P_0	1371	1307	$\pi(1300)$	1300 ± 100
1^-1^{-+}	1^3P_1	1371	1307	$\pi_1(1400)$	1354 ± 25
1^-1^{-+}	1^5F_1	1775	1691	$\pi_1(1600)$	1662^{+15}_{-11}
1^+1^{--}	1^1P_1	1580	1558	$\rho(1570)$	$1570 \pm 36 \pm 62$
1^+1^{--}	1^5F_1	2157	2030	$\rho(2150)$	2149 ± 17
1^+3^{--}	1^5P_3	1697	1651	$\rho_3(1690)$	1686 ± 4
1^+3^{--}	2^5P_3	2146	2062	$\rho_3(1990)$	1982 ± 14
1^+1^{+-}	1^3S_1	1070	1089	$b_1(1235)$	1229.5 ± 3.2
2^+0^{++}	1^1S_0	1202	1211	<i>exotic</i>	...
2^+0^{++}	1^3P_0	1655	1617	<i>exotic</i>	...
2^-1^{--}	1^1P_1	1580	1558	<i>exotic</i>	...
2^-1^{--}	1^5P_1	1697	1651	<i>exotic</i>	...
2^-1^{+-}	1^3S_1	1388	1391	<i>exotic</i>	...
2^+1^{++}	1^5D_1	1927	1840	<i>exotic</i>	...
2^+2^{++}	1^1D_2	1876	1807	<i>exotic</i>	...
2^+2^{++}	1^5S_2	1468	1470	<i>exotic</i>	...

The tetraquark states in the flux-tube model are generally lower than that in the traditional quark models with additive two-body confinement interaction with color factors used in early multiquark state calculations [50,74]. The reason for this is that the multibody confinement

TABLE II. The mass spectra for $ns\bar{n}\bar{s}$ states.

$I^G J^{PC}$	$N^{2S+1}L_J$	E_I	E_{II}	States	PDG
0^+0^{++}	1^1S_0	1316	1318	$f_0(1370)$	1200–1500
0^+0^{++}	2^1S_0	1583	1590	$f_0(1500)$	1505 ± 6
0^+0^{++}	3^1S_0	1676	1661	$f_0(1710)$	1720 ± 6
0^+0^{++}	1^5D_0	2174	2095	$f_0(2100)$	2103 ± 8
0^+0^{++}	1^5D_0	2174	2095	$f_0(2200)$	2189 ± 13
0^+2^{++}	1^5S_2	1751	1755	$f_2(1810)$	1815 ± 12
0^+2^{++}	1^1D_2	2033	1946	$f_2(2010)$	2011^{+62}_{-76}
0^+2^{++}	2^1D_2	2141	2073	$f_2(2150)$	2157 ± 12
0^+2^{++}	1^5D_2	2174	2095	$f_2(2150)$	2157 ± 12
0^+0^{-+}	1^3P_0	1867	1831	$\eta(1760)$	1756 ± 9
0^+2^{-+}	1^3P_2	1867	1831	$\eta_2(1870)$	1842 ± 8
0^-1^{--}	1^1P_1	1773	1740	$\phi(1680)$	1680 ± 20
0^-1^{--}	2^1P_1	1892	1866
0^-1^{+-}	1^3S_1	1583	1586	$h_1(1595)$	$1594 \pm 15^{+10}_{-60}$
0^-1^{+-}	2^3S_1	1626	1628
0^+1^{-+}	1^3P_1	1865	1828	<i>exotic</i>	...
0^-2^{+-}	1^3D_2	2108	2076	<i>exotic</i>	...
0^-3^{--}	1^5P_3	1968	1928	$\phi_3(1850)$	1854 ± 7
1^-0^{++}	1^1S_0	1320	1318	$a_0(980)$	980 ± 20
1^-0^{++}	2^1S_0	1584	1590	$a_0(1450)$	1474 ± 19
1^-2^{++}	1^5S_2	1751	1755	$a_2(1700)$	1732 ± 16
1^-2^{++}	1^1D_2	2033	1945
1^-0^{-+}	1^3P_0	1867	1831	$\pi(1800)$	1816 ± 14
1^-1^{-+}	1^3P_1	1867	1831	<i>exotic</i>	...
1^-2^{+-}	1^3D_2	2108	2076	<i>exotic</i>	...
1^-2^{-+}	1^3P_2	1867	1831	$\pi_2(1880)$	1895 ± 16
1^-2^{-+}	1^3F_2	2309	2186	$\pi_2(2100)$	2090 ± 29
1^+1^{--}	1^1P_1	1772	1739	$\rho(1700)$	1700 ± 20
1^+1^{--}	2^1P_1	1892	1866	$\rho(1900)$	$1909 \pm 17 \pm 25$
1^+1^{--}	1^5F_5	2376	2259	$\rho(2150)$	2149 ± 17
1^+3^{--}	1^5P_3	1967	1928	$\rho_3(1990)$	1982 ± 14
1^+3^{--}	1^1F_3	2248	2117	$\rho_3(2250)$	~ 2232
1^+5^{--}	1^5F_5	2376	2259	$\rho_5(2350)$	2330 ± 35
1^-1^{+-}	1^5D_1	2173	2095
1^+1^{+-}	1^3S_1	1583	1586

TABLE III. The mass spectra for $ss\bar{s}\bar{s}$ states.

$I^G J^{PC}$	$N^{2S+1}L_J$	E_I	E_{II}	States	PDG
0^+0^{++}	1^1S_0	1919	1925	$f_0(2020)$	1992 ± 16
0^+0^{++}	1^5D_0	2440	2365	$f_0(2330)$	2314 ± 25
0^+2^{++}	1^5S_2	2051	2044	$f_2(2010)$	2011^{+62}_{-76}
0^+2^{++}	1^1D_2	2423	2354	$f_2(2300)$	2297 ± 28
0^+2^{++}	1^5D_2	2440	2365	$f_2(2300)$	2297 ± 28
0^+2^{++}	1^1D_2	2423	2354	$f_2(2340)$	2340 ± 55
0^+2^{++}	1^5D_2	2440	2365	$f_2(2340)$	2340 ± 55
0^+4^{++}	1^5D_2	2440	2365	$f_4(2300)$	~ 2314
0^-1^{--}	1^1P_1	2201	2176	$\phi(2170)$	2175 ± 15
0^+0^{-+}	1^3P_0	2232	2195	$\eta(2225)$	2226 ± 16
0^-1^{--}	1^5P_1	2249	2209	$\phi(2170)$	2175 ± 15
0^-1^{+-}	1^3D_1	2432	2359

TABLE IV. The mass spectra for $nn\bar{n}\bar{s}$ states.

IJ^P	$N^{2S+1}L_J$	E_I	E_{II}	States	PDG
1^+0^+	1^1S_0	995	947	$K_0^*(800)$	676 ± 40
1^+0^+	2^1S_0	1383	1380	$K_0^*(1430)$	1425.6 ± 1.5
1^+0^+	1^5D_0	2050	1968	$K_0^*(1950)$	$1945 \pm 10 \pm 20$
1^+2^+	1^5D_2	2050	1968	$K_2^*(1980)$	$1973 \pm 8 \pm 25$
1^+4^+	1^5D_4	2050	1968	$K_4^*(2045)$	2045 ± 9
1^+0^-	1^3P_0	1514	1451	$K(1460)$	~ 1460
1^+0^-	2^3P_0	1739	1697	$K(1630)$	1629 ± 7
1^+0^-	3^3P_0	1772	1754	$K(1830)$	~ 1830
1^-1^-	1^1P_1	1430	1367	$K^*(1410)$	1414 ± 15
1^-1^-	2^1P_1	1709	1666	$K^*(1680)$	1717 ± 27
1^+1^+	1^3S_1	1254	1233	$K_1(1270)$	1272 ± 7
1^+1^+	2^3S_1	1447	1456	$K_1(1400)$	1403 ± 7
1^+1^+	1^3D_1	1749	1644	$K_1(1650)$	1650 ± 50
1^+2^+	1^5S_2	1603	1601	$K_2^*(1430)$	1425.6 ± 1.5
1^+2^+	1^1D_2	1685	1573	$K_2^*(1430)$	1425.6 ± 1.5
1^+2^+	2^1D_2	2014	1942	$K_2^*(1980)$	$1973 \pm 8 \pm 25$
1^+2^-	1^3P_2	1514	1451	$K_2(1580)$	~ 1580
1^+2^-	1^5P_2	1828	1786	$K_2(1770)$	1773 ± 8
1^+2^-	1^5P_2	1828	1786	$K_2(1820)$	1816 ± 13
1^+3^-	1^5P_3	1828	1786	$K_3^*(1780)$	1776 ± 7

potential can avoid the appearance of anticonfinement in a color symmetric quark or antiquark pair. From Tables I, II, III, IV, and V, it can be seen that the two structures generally give very close energies for tetraquark ground states. However, the differences between two structures are about 40 MeV, 80 MeV and 120 MeV for spatial excitations between Q and \bar{Q} with $L = 1$, $L = 2$ and $L = 3$, respectively, which is attributed to the following: (i) the expected values of the quadratic confinement potentials which linearly depend on the angular excitation L [71]; (ii) different normal modes due to three different independent quadratic confinement potentials of two flux-tube structures [see

TABLE V. The mass spectra for $ns\bar{s}\bar{s}$ states.

IJ^P	$N^{2S+1}L_J$	E_I	E_{II}	States	PDG
1^+0^+	1^1S_0	1757	1762
1^+0^+	2^1S_0	1938	1945	$K_0^*(1950)$	$1945 \pm 10 \pm 20$
1^+3^+	1^5D_3	2308	2230	$K_3(2320)$	2324 ± 24
1^+0^-	1^3P_0	2026	1984
1^+0^-	2^3P_0	2088	2051
1^-1^-	1^1P_1	2051	2024
1^-1^-	2^1P_1	2160	2139
1^-2^-	1^5P_2	2108	2068	$K_2^*(2250)$	2247 ± 17
1^-4^-	1^5F_4	2503	2386	$K_4^*(2500)$	2490 ± 20
1^-5^-	1^5F_5	2503	2386	$K_5^*(2380)$	$2382 \pm 14 \pm 19$
1^+1^+	1^3S_1	1778	1774
1^+1^+	2^3S_1	1864	1862
1^+2^+	1^5S_2	1904	1900
1^+2^+	1^1D_2	2284	2215
1^+2^+	2^1D_2	2440	2386

Eqs. (7) and (8)]. For a compact tetraquark state in the ground state, the separation among particles (quarks or antiquarks) is generally smaller than 1 fm [49], so the square of the length of each flux tube is smaller than the length itself. It is therefore predicted that the small difference of the same quantum state between a linear confinement and a quadratic one is about 50–80 MeV according to the calculations on hexaquark states [48]. Anyway, the differences of the ground states between two structures are not big for both the linear and quadratic confinement potentials.

In general, a tetraquark system should be the mixture of all possible flux-tube structures. Such as in the process of meson-meson scattering, when two color singlet mesons are separated far away, the dominant component of the system should be two isolated color singlet mesons because other hidden color flux-tube structures are suppressed due to the confinement. With the separation reduction, a deuteron-like meson-meson molecular state may be formed if the attractive force between two color singlet mesons is strong enough. When they are close enough to be within the range of confinement (about 1 fm), all possible flux-tube structures including the QCD quark cyclobutadiene and even more complicated flux-tube structures may appear due to the excitation and rearrangements of flux tubes and junctions. All of these hidden color components cannot directly decay into two colorful hadrons due to the color confinement. They must transform back into two color singlet mesons by means of the rupture and recombination of flux tubes before decaying into two color singlet mesons. The decay widths of these states are qualitatively determined by the speed of the rupture and recombination of the flux tubes. These formation and decay mechanisms are similar to the compound nucleus formation and therefore should induce a resonance called a “color confined, multi-quark resonance” state [75]. It is different from all of those microscopic resonances discussed by Weinberg [76]. Bicudo and Cardoso studied tetraquark states using the triple flip-flop potential including two meson-meson potentials and the tetraquark four-body potential. They also found it plausible that there exist resonances in which the tetraquark component originated by a flip-flop potential is the dominant one [77].

Most tetraquark states in Tables I, II, III, IV, and V have the same quantum numbers as ordinary meson states, and the calculated energies of many tetraquark states are very close to the experimental data of the mesons with the same quantum numbers [78], especially states with higher energy. This does not mean that the main component of those experimental states must be tetraquark states. The fact is that most of the experimentally observed mesons can be interpreted as $q\bar{q}$ states (at least the main component) and accommodated in the naive quark model; only a few of them may go beyond $q\bar{q}$ configurations [79,80]. However, the calculations indicate that the tetraquark component in

those mesons (their energies are close to the tetraquark ones) cannot be excluded. This point is supported by the study on the nature of scalar mesons [4–10]. Moreover the nucleon spin structure study shows that, even for the ground state, the pentaquark component $q^3q\bar{q}$ is indispensable in solving the proton spin “crisis” [81,82]. The strange magnetic momentum of a nucleon originating from a strange sea quark $s\bar{s}$ component is nonzero [83]. So a comprehensive study of the meson spectra must include the mixing of $q\bar{q}$ and $q^2\bar{q}^2$ Fock components and, in turn, requires the knowledge of the off-shell interaction for annihilating or creating a quark-antiquark pair into or from the vacuum. The quark model should be unquenched, and such an unquenched quark model study is ongoing in our group.

With regard to nonstrange mesons, for some light $q\bar{q}$ excitation states, the orbital excitation energy between q and \bar{q} may be higher than that of a quark-antiquark pair excited from the quark sea, so these meson states prefer to have the high Fock component $q^2\bar{q}^2$. Like the meson σ , it can be described as a ground state with the quark content $n^2\bar{n}^2$ rather than excited states of a $q\bar{q}$ meson [50], which is consistent with many other works [5,7–9,44,84–86]. The first radial excited state of the $n^2\bar{n}^2$ state is very close to the experimental value of the meson $f_0(980)$; the tetraquark state $n^2\bar{n}^2$ may therefore be one of the main components, which is supported by the work on the nature of scalar mesons [6,10]. The decay of the meson $f_0(980)$ into $K\bar{K}$ can be accounted for by other strangeness components, such as $s\bar{s}$ and $ns\bar{n}\bar{s}$. The meson $f_0(1500)$ cannot be described as a $q\bar{q}$ meson; the mass and decay are compatible with it being the ground state glueball mixed with the nearby states of the 0^{++} $\bar{q}q$ nonet [80]. In the quark models, another interpretation of the meson $f_0(1500)$ is that the main component might be a tetraquark state $ns\bar{n}\bar{s}$ [10]. The meson $f_2(1430)$ has no proper member in the $q\bar{q}$ picture [79]. It is suggested that the main component is a tetraquark $n^2\bar{n}^2$ with quantum numbers 1^5S_2 in the flux-tube model. This state has not been confirmed by the PDG, and even recent measurements have suggested a different assignment of quantum numbers, which could make it compatible with the lightest scalar glueball [87].

With respect to $I = \frac{1}{2}$ strange mesons, most of them can be interpreted as dominated by $q\bar{q}$ components in the quark models except for three mesons, $\kappa(800)$, $K^*(1410)$ and $K_2(1580)$ [79]. For the same reason as with the meson σ , our model recommends a ground tetraquark state $n^2\bar{n}\bar{s}$ 1^1S_0 with energy close to the meson $\kappa(800)$, which is compatible with other works [6–9,44,84–86]. For the meson $K^*(1410)$, its assignment to the 2^3S_1 state of the meson $K^*(892)$ is excluded not only by the large mass difference, but also by its decay modes [79]. A possible interpretation of the main component of this state is a tetraquark state $n^2\bar{n}\bar{s}$ with quantum numbers 1^1P_1 instead of a pure $q\bar{q}$ pair. The meson $K_2(1580)$ also has no proper member in

the $q\bar{q}$ spectra [79]; our tetraquark state 1^3P_2 mass is a little lower than experimental data. This state is clearly uncertain; it was reported in only one experimental work more than 20 years ago and has never been measured again.

Concerning the exotic meson sector, the quantum numbers rule out the pure $q\bar{q}$ possibility. The π_1 mesons of $I^G J^{PC} = 1^- 1^{-+}$ are listed as manifestly exotic states by several experiments [88–91]. Many theoretical studies have been made, and various interpretations were proposed: hybrid meson states [92–95], $\pi\eta$ molecular states [96] and tetraquark states [97,98]. Two mesons, $\pi_1(1400)$ and $\pi_1(1600)$, are studied in the flux-tube model (see Table I), which indicates that the main components of $\pi_1(1400)$ and $\pi_1(1600)$ might be tetraquark states $n^2\bar{n}^2$ with quantum numbers 1^3P_1 and 1^5F_1 , respectively. The tetraquark states $ns\bar{n}\bar{s}$ with quantum numbers $I = 0, 1$ and $J^{PC} = 1^{-+}$ are predicted in the flux-tube model; the energies are around 1850 MeV (see Table II), which is consistent with the predictions on $J^{PC} = 1^{-+}$ tetraquark states in the QCD sum rule [97,98]. The exotic meson states with quantum numbers $J^{PC} = 2^{+-}$ are predicted in the tetraquark picture; the states $n^2\bar{n}^2$ and $ns\bar{n}\bar{s}$ have the lowest masses, around 1880 MeV and 2100 MeV, respectively. In addition, many flavor $I = 2$ exotic meson states are also calculated for further studies (see Table I).

VI. SUMMARY

The QCD quark cyclobutadiene, a new flux-tube structure, is proposed in the framework of the flux-tube model. The flux-tube ring in the QCD quark cyclobutadiene can be described as a glueball; four quarks are connected to the flux-tube ring by four fundamental flux tubes, and thus the QCD quark cyclobutadiene can be viewed as a $q^2\bar{q}^2$ -glueball hybrid. It provides a new sample for understanding the structures of exotic hadrons. The three familiar flux-tube structures ($[[q\bar{q}]_1[q\bar{q}]_1]$, $[[qq]_3[\bar{q}\bar{q}]_3]_1$ and $[[q\bar{q}]_8[q\bar{q}]_8]_1$) can be taken as the ground states of a tetraquark system. The QCD quark cyclobutadiene may be an excited state which is obtained by means of creating Y-shaped junctions and flux tubes from the vacuum and the rearrangement of some flux tubes. The QCD quark cyclobutadiene and three other flux tube structures are QCD isomeric compounds due to the same quark component and different flux-tube structures.

Most meson states from the PDG can be described as $q\bar{q}$ configurations; only a few meson states, σ , $\kappa(800)$, $f_0(980)$, $f_0(1500)$, $\pi_1(1400)$, $\pi_1(1600)$, $f_2(1430)$ and $K^*(1410)$, are difficult to be interpreted as $q\bar{q}$ meson states. The tetraquark states as their main components is one of the possible interpretations of their flavor components. Some exotic meson states as tetraquark states are predicted in the flux-tube model. The tetraquark states $ns\bar{n}\bar{s}$ with quantum numbers $I = 0, 1$ and $J^{PC} = 1^{-+}$ have the lowest masses around 1850 MeV. The tetraquark states $n^2\bar{n}^2$ and $ns\bar{n}\bar{s}$ with quantum numbers $J^{PC} = 2^{+-}$ have the lowest

masses around 1880 MeV and 2100 MeV, respectively. The tetraquark states with $I = 2$ are also predicted in the flux-tube model.

Even though up to now no tetraquark state has been well established experimentally, it is indispensable to continue the study of the tetraquark system because the tetraquark component in mesons cannot be ruled out and may play an important role in the properties of mesons, similar to the fact that the pentaquark components play an important role even in the nucleon ground state.

The tetraquark states, if they really exist, should be mixtures of all kinds of flux-tube structures which can transform one another. In this way, the flip-flop of flux-tube structures can induce a resonance which is called a “color confined, multiquark resonance” state. To verify

such a new resonance is not easy. We admit that this analysis is based on the mass calculation only; the crucial test of the components of exotic mesons is determined by the systematic study of their decays, which involves a channel coupling calculation containing all possible flux-tube structures and mixing between $q\bar{q}$ and tetraquark components, and so much more information of low energy QCD is needed.

ACKNOWLEDGMENTS

This work is supported partly by the National Science Foundation of China under Grants No. 11047140, No. 11035006, and No. 11175088, and the Ph.D Program Funds of Chongqing Jiaotong University.

-
- [1] S. Godfrey and J. Napolitano, *Rev. Mod. Phys.* **71**, 1411 (1999).
 - [2] C. Amsler and N. A. Törnqvist, *Phys. Rep.* **389**, 61 (2004).
 - [3] R. L. Jaffe, *Phys. Rep.* **409**, 1 (2005).
 - [4] D. Black, A. H. Fariborz, and J. Schechter, *Phys. Rev. D* **61**, 074001 (2000).
 - [5] A. H. Fariborz, *Int. J. Mod. Phys. A* **19**, 2095 (2004).
 - [6] M. Napsuciale and S. Rodriguez, *Phys. Rev. D* **70**, 094043 (2004).
 - [7] A. H. Fariborz, R. Jora, and J. Schechter, *Phys. Rev. D* **72**, 034001 (2005).
 - [8] F. Giacosa, *Phys. Rev. D* **74**, 014028 (2006).
 - [9] F. Giacosa, *Phys. Rev. D* **75**, 054007 (2007).
 - [10] J. Vijande, A. Valcarce, F. Fernandez, and B. Silvestre-Brac, *Phys. Rev. D* **72**, 034025 (2005).
 - [11] B. Aubert *et al.* (BABAR Collaboration), *Phys. Rev. Lett.* **90**, 242001 (2003).
 - [12] S. K. Choi *et al.* (Belle Collaboration), *Phys. Rev. Lett.* **91**, 262001 (2003).
 - [13] A. V. Evdokimov *et al.* (SELEX Collaboration), *Phys. Rev. Lett.* **93**, 242001 (2004).
 - [14] D. R. Thompson *et al.* (E852 Collaboration), *Phys. Rev. Lett.* **79**, 1630 (1997).
 - [15] A. Abele *et al.* (Crystal Barrel Collaboration), *Phys. Lett. B* **446**, 349 (1999).
 - [16] G. S. Adams *et al.* (E862 Collaboration), *Phys. Lett. B* **657**, 27 (2007).
 - [17] M. G. Alekseev *et al.* (COMPASS Collaboration), *Phys. Rev. Lett.* **104**, 241803 (2010).
 - [18] F. Nerling *et al.* (COMPASS Collaboration), [arXiv:1208.0474](https://arxiv.org/abs/1208.0474).
 - [19] C. Y. Wong, *Phys. Rev. C* **69**, 055202 (2004).
 - [20] F. E. Close and P. R. Page, *Phys. Lett. B* **578**, 119 (2004).
 - [21] E. S. Swanson, *Phys. Lett. B* **588**, 189 (2004).
 - [22] N. A. Törnqvist, *Phys. Lett. B* **590**, 209 (2004).
 - [23] L. Maiani, F. Piccinini, A. D. Polosa, and V. Riquer, *Phys. Rev. D* **71**, 014028 (2005).
 - [24] H. Hogaasen, J. M. Richard, and P. Sorba, *Phys. Rev. D* **73**, 054013 (2006).
 - [25] D. Ebert, R. N. Faustov, and V. O. Galkin, *Phys. Lett. B* **634**, 214 (2006).
 - [26] N. Barnea, J. Vijande, and A. Valcarce, *Phys. Rev. D* **73**, 054004 (2006).
 - [27] J. Vijande, E. Weissman, N. Barnea, and A. Valcarce, *Phys. Rev. D* **76**, 094022 (2007).
 - [28] D. Janc and M. Rosina, *Few-Body Syst.* **35**, 175 (2004).
 - [29] S. L. Olson, *Nucl. Phys.* **A827**, 53c (2009), and references therein.
 - [30] H. X. Chen, A. Hosaka, and S. L. Zhu, *Phys. Rev. D* **78**, 054017 (2008).
 - [31] C. K. Jiao, W. Chen, H. X. Chen, and S. L. Zhu, *Phys. Rev. D* **79**, 114034 (2009).
 - [32] J. J. Dudek, R. G. Edwards, M. J. Peardon, D. G. Richards, and C. E. Thomas, *Phys. Rev. Lett.* **103**, 262001 (2009).
 - [33] V. Dmitrasinovic, *Phys. Rev. D* **67**, 114007 (2003).
 - [34] C. Alexandrou, P. De Forcrand, and A. Tsapalis, *Phys. Rev. D* **65**, 054503 (2002).
 - [35] T. T. Takahashi, H. Suganuma, Y. Nemoto, and H. Matsufuru, *Phys. Rev. D* **65**, 114509 (2002).
 - [36] F. Okiharu, H. Suganuma, and T. T. Takahashi, *Phys. Rev. D* **72**, 014505 (2005).
 - [37] F. Okiharu, H. Suganuma, and T. T. Takahashi, *Phys. Rev. Lett.* **94**, 192001 (2005).
 - [38] P. W. Anderson, *Phys. Today* **53**, No. 2, 11 (2000).
 - [39] F. Wang, G. H. Wu, L. J. Teng, and T. Goldman, *Phys. Rev. Lett.* **69**, 2901 (1992).
 - [40] T. Barnes, F. E. Close, and H. J. Lipkin, *Phys. Rev. D* **68**, 054006 (2003).
 - [41] I. W. Lee, A. Faessler, T. Gutsche, and V. E. Lyubovitskij, *Phys. Rev. D* **80**, 094005 (2009).
 - [42] X. Liu, X. Q. Zeng, and X. Q. Li, *Phys. Rev. D* **72**, 054023 (2005).
 - [43] R. L. Jaffe and F. Wilczek, *Phys. Rev. Lett.* **91**, 232003 (2003).

- [44] L. Maiani, F. Piccinini, A. D. Polosa, and V. Riquer, *Phys. Rev. Lett.* **93**, 212002 (2004).
- [45] D. Ebert, R. N. Faustov, V. O. Galkin, and W. Lucha, *Phys. Rev. D* **76**, 114015 (2007).
- [46] H. X. Huang, C. R. Deng, J. L. Ping, F. Wang, and T. Goldman, *Phys. Rev. C* **77**, 025201 (2008).
- [47] J. L. Ping, H. X. Huang, C. R. Deng, F. Wang, and T. Goldman, *Phys. Rev. C* **79**, 065203 (2009).
- [48] J. L. Ping, C. R. Deng, F. Wang, and T. Goldman, *Phys. Lett. B* **659**, 607 (2008).
- [49] C. R. Deng, J. L. Ping, Y. C. Yang, and F. Wang, *Phys. Rev. D* **86**, 014008 (2012).
- [50] C. R. Deng, J. L. Ping, F. Wang, and T. Goldman, *Phys. Rev. D* **82**, 074001 (2010).
- [51] N. Isgur and J. Paton, *Phys. Rev. D* **31**, 2910 (1985).
- [52] G. S. Bali, *Phys. Rev. D* **62**, 114503 (2000).
- [53] Y. Koma, H. Suganuma, and H. Toki, *Phys. Rev. D* **60**, 074024 (1999).
- [54] P. Maris and C. R. Roberts, *Int. J. Mod. Phys. E* **12**, 297 (2003).
- [55] N. Ishii, S. Aoki, and T. Hatsuda, *Phys. Rev. Lett.* **99**, 022001 (2007).
- [56] T. T. Takahashi and Y. Kanada-En'yo, *Phys. Rev. D* **82**, 094506 (2010).
- [57] T. Inoue, N. Ishii, S. Aoki, T. Doi, T. Hatsuda, Y. Ikeda, K. Murano, H. Nemura, and K. Sasaki (HAL QCD Collaboration), *Phys. Rev. Lett.* **106**, 162002 (2011).
- [58] N. Ishii, *AIP Conf. Proc.* **1355**, 206 (2011).
- [59] G. Feinberg and J. Sucher, *Phys. Rev. D* **20**, 1717 (1979).
- [60] O. W. Greenberg and H. J. Lipkin, *Nucl. Phys.* **A370**, 349 (1981).
- [61] J. Weinstein and N. Isgur, *Phys. Rev. Lett.* **48**, 659 (1982).
- [62] J. Weinstein and N. Isgur, *Phys. Rev. D* **41**, 2236 (1990).
- [63] M. Oka, *Phys. Rev. D* **31**, 2274 (1985).
- [64] M. Oka and C. J. Horowitz, *Phys. Rev. D* **31**, 2773 (1985).
- [65] M. Karliner and H. J. Lipkin, *Phys. Lett. B* **575**, 249 (2003).
- [66] J. Vijande, A. Valcarce, and J. M. Richard, *Phys. Rev. D* **76**, 114013 (2007).
- [67] F. Wang and C. W. Wong, *Nuovo Cimento A* **86**, 283 (1985).
- [68] T. Goldman and S. Yankielowicz, *Phys. Rev. D* **12**, 2910 (1975).
- [69] M. Iwasaki, S. Nawa, T. Sanada, and F. Takagi, *Phys. Rev. D* **68**, 074007 (2003).
- [70] J. Carlson and V. R. Pandharipande, *Phys. Rev. D* **43**, 1652 (1991).
- [71] E. Hiyama, Y. Kino, and M. Kamimura, *Prog. Part. Nucl. Phys.* **51**, 223 (2003).
- [72] F. J. Llanes-Estrada, in *Workshop on e^+e^- in the 1–2 GeV range, Alghero, Italy, 2003*, econf c0309101, FRWP011 (2003).
- [73] E. Santopinto and G. Galatà, *Phys. Rev. C* **75**, 045206 (2007).
- [74] C. R. Deng, J. L. Ping, and F. Wang, [arXiv:1202.4169](https://arxiv.org/abs/1202.4169) [Chin. Phys. C (to be published)].
- [75] F. Wang, J. L. Ping, H. R. Pang, and L. Z. Chen, *Nucl. Phys.* **A790**, 493c (2007).
- [76] S. Weinberg, *The Quantum Theory of Fields* (Cambridge University Press, Cambridge, England, 1995), Vol. I, p. 159.
- [77] P. Bicudo and M. Cardoso, *Phys. Rev. D* **83**, 094010 (2011).
- [78] K. Nakamura *et al.* (Particle Data Group), *J. Phys. G* **37**, 075021 (2010).
- [79] J. Vijande, F. Fernandez, and A. Valcarce, *J. Phys. G* **31**, 481 (2005).
- [80] E. Klempt and A. Zaitsev, *Phys. Rep.* **454**, 1 (2007).
- [81] D. Qing, X. S. Chen, and F. Wang, *Phys. Rev. C* **57**, R31 (1998).
- [82] D. Qing, X. S. Chen, and F. Wang, *Phys. Rev. D* **58**, 114032 (1998).
- [83] B. S. Zou and D. O. Riska, *Phys. Rev. Lett.* **95**, 072001 (2005).
- [84] M. G. Alford and R. L. Jaffe, *Nucl. Phys.* **B578**, 367 (2000).
- [85] J. R. Pelaez, *Phys. Rev. Lett.* **92**, 102001 (2004).
- [86] J. R. Pelaez and G. Rios, *Phys. Rev. Lett.* **97**, 242002 (2006).
- [87] C. J. Morningstar and M. Peardon, *Phys. Rev. D* **60**, 034509 (1999).
- [88] M. Lu *et al.* (E852 Collaboration), *Phys. Rev. Lett.* **94**, 032002 (2005).
- [89] W. M. Yao *et al.* (Particle Data Group), *J. Phys. G* **33**, 1 (2006).
- [90] G. S. Adams *et al.* (E852 Collaboration), *Phys. Lett. B* **657**, 27 (2007).
- [91] M. Nozar *et al.* (CLAS Collaboration), *Phys. Rev. Lett.* **102**, 102002 (2009).
- [92] P. R. Page, E. S. Swanson, and A. P. Szczepaniak, *Phys. Rev. D* **59**, 034016 (1999).
- [93] K. G. Chetyrkin and S. Narison, *Phys. Lett. B* **485**, 145 (2000).
- [94] H. Y. Jin, J. G. Korner, and T. G. Steele, *Phys. Rev. D* **67**, 014025 (2003).
- [95] C. Bernard, T. Burch, E. Gregory, D. Toussaint, C. DeTar, J. Osborn, S. Gottlieb, U. Heller, and R. Sugar, *Phys. Rev. D* **68**, 074505 (2003).
- [96] R. Zhang, Y. B. Ding, X. Q. Li, and P. R. Page, *Phys. Rev. D* **65**, 096005 (2002).
- [97] H. X. Chen, A. Hosaka, and S. L. Zhu, *Phys. Rev. D* **78**, 054017 (2008).
- [98] H. X. Chen, A. Hosaka, and S. L. Zhu, *Phys. Rev. D* **78**, 117502 (2008).